

CLARITY Registration Report

Kwame Sanwu Kutten, Michael I. Miller, Joshua Vogelstein

Objective

1. Learn more about mouse neuroanatomy
2. Learn more about whole brain CLARITY registrations
3. Learn about non-linear registration on these kinds of data
4. Build towards a CLARITY registration Web-service, where anybody with CLARITY data can upload their data, and various atlases are automatically registered to each brain

Methods

1. Built linear, affine, and nonlinear registration, both on images and on brain masks (ignoring all the interior of the brain)
2. Compared with Raju method
3. Use several metrics to assess accuracy, including mutual information, median surface distance, median landmark error, and visual inspection
4. 3 different kinds of comparisons: CLARITY to ABA, within condition CLARITY, across condition CLARITY

Results

1. Nonlinear brain mask registration works best when registering CLARITY to ABA, which is expected, as the images are highly divergent. This is obvious upon visual inspection of the registrations.
2. Nonlinear image registration works best when registering CLARITY to CLARITY.

Next Steps

1. Get feedback from Stanford crew on this report (you can visually inspect the data in 3D using ITK by following the instructions in Appendix A).
2. Enable Web-viz with overlays in native orientation (< 1 week)
3. Enable Web-viz in sagittal planes with overlaid atlases (< 1 month)
4. Make open source package for 1-click CLARITY registration (< 1 month)
5. Make ingest and registration into a Web-service (< 2 months)
6. Improve algorithms by incorporating automatically detected interior landmarks, such as the corpus callosum and/or ventricles.

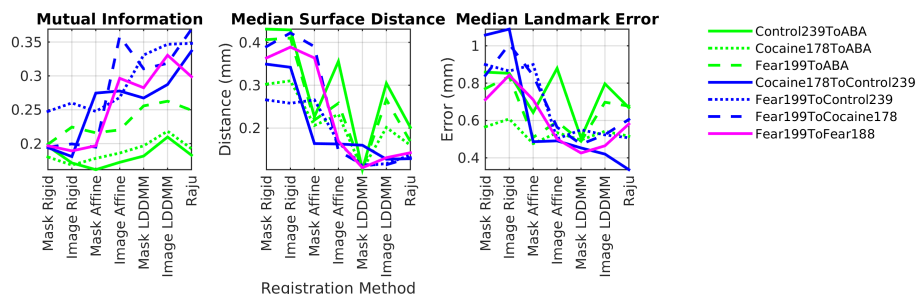


Figure 1: Registraton Results Summary

1 Methods

1.1 Data

The Allen Mouse Brain Atlas (ABA), a Nissl stained volume with corresponding labels, was downloaded at a $25 \mu\text{m}$ isotropic resolution from the Allen Brain Institute [1]. Four CLARITY images (Control239, Cocaine178, Fear188, Fear199) were downloaded using the OCP API and resampled to a $25 \mu\text{m}$ isotropic resolution. Brain masks were created for each CLARITY image using the following procedure: First rough brain masks were generated by manually thresholding each CLARITY image. Next the brain masks were morphologically opened using a $50 \mu\text{m}$ ball-shaped kernel to remove small objects in the background. These masks were then morphologically closed using a $125 \mu\text{m}$ kernel to remove large holes in the foreground.

1.2 Registration Methods

Two registration pipelines were developed, and image based pipeline, and a mask based pipeline.

In the *Image-LDDMM Pipeline*, images were registered directly to each other. Preprocessing consisted of two steps. First the brain masks were applied to the images. Next the masked template image was histogram matched to the target image using the *Insight Segmentation and Registration Toolkit* (ITK) [4]. In the matching procedure, 32-bin histograms were calculated for both the template and target images. The histograms were matched exactly at 8 quantile points and by interpolation at all other intensities between these points. Registration was then done with a three step process with (1) Rigid, (2) Affine and (3) Deformable transforms.

Let $\Omega \subset \mathbb{R}^3$ be the background space. Let $I_0 : \Omega \rightarrow \mathbb{R}$ be the template image which will be deformed to match target image $I_1 : \Omega \rightarrow \mathbb{R}$.

1. Rigid transforms between, I_0 and I_1 were computed using a custom MATLAB script written by Daniel Tward of JHU.
2. Affine transforms (12 parameter) were computed using the open source *Automated Image Registration* (AIR) toolkit. The cost function, a least squares difference between the transformed template and target images, was minimized using Newton's Method [2].
3. Deformable registration was done using the *Large Deformation Diffeomorphic Metric Mapping* (LDDMM) algorithm. It is a fluid registration method used to compute smooth invertible transforms between images. Let $v : [0, 1] \times \Omega \rightarrow \mathbb{R}^3$ be the velocity of the flow so that $\varphi = \int_0^1 v(t, \varphi) dt$ is the displacement. LDDMM minimizes the objective function

$$E(v) = \int_0^1 \|Kv(t)\|_{L_2}^2 dt + \frac{1}{\sigma^2} \|I_0 \circ \varphi^{-1} - I_1\|_{L_2}^2$$

where K is a kernel which ensures that v is sufficiently smooth and $\sigma = 1$ in our experiments [3].

In the *Mask-LDDMM Pipeline* no preprocessing was necessary. The brain masks were registered to each other using the same three step procedure.

1.3 Registration Evaluation

The registrations were quantitatively evaluated using three methods. Let φ be the computed transform from template to target space. Let I_0 and I_1 be the template and target images. Let T and U be random variables denoting the intensities of the deformed template $I(1) = I_0 \circ \varphi^{-1}$ and target I_1 images respectively. The *Mutual Information (MI)* between the template and target images is

$$\begin{aligned} MI(T, U) &= H(T) + H(U) - H(T, U) \\ &= \iint_{\Omega} p(t, u) \ln \left(\frac{p(t, u)}{p(t)p(u)} \right) dt du \end{aligned}$$

Where $p(t)$, $p(u)$ and $p(t, u)$ are the deformed template histogram, target histogram, and joint histogram respectively.

Computing MI directly may yield unstable results. Therefore it was estimated using the *Viola-Wells* method, as implemented in ITK [4]. In this method, densities $p(t)$, $p(u)$ and $p(t, u)$ were estimated from 1000 samples using a Gaussian distribution based Parzen Window. These results were graphed in Fig. 2b-8b.

We also used landmark based methods to evaluate the results. Specifically, $N = 55$ landmarks were chosen and placed on the ABA and CLARITY images using MRIStudio's DiffeoMap program. Of the landmarks, 28 were placed on the surface of the brain while the remaining 27 were placed on internal structures. Let x_k and y_k be the positions of the k^{th} template and target landmarks where $k \in \{1, \dots, N\}$. The *error in position of the k^{th} landmark* after registration is

$$e_k = d(\varphi(x_k), y_k) = \|\varphi(x_k) - y_k\|_{L_2}$$

In Fig 2c-8c these errors are displayed as notched boxplots.

Let M_0 and M_1 be the template and target masks respectively. Let $S(1) = \partial(M_0 \circ \varphi^{-1})$ denote the surface of the deformed template. Let $S_1 = \partial M_1$ denote the surface of the target. The *Hausdorff Distance (HD)* between the deformed template and target surfaces is defined as

$$d_H(S(1), S_1) = \max \left\{ \sup_{x \in S(1)} \inf_{y \in S_1} d(x, y), \sup_{y \in S_1} \inf_{x \in S(1)} d(x, y) \right\}$$

Since the Hausdorff Distance is a maximum distance between the surfaces, it does not give information on the spread of these distances over the surfaces. Therefore for every point in the deformed template, $x \in S(1)$, the distance between it and the target surface, $\inf_{y \in S_1} d(x, y)$, was computed. Likewise for every point in the target $y \in S_1$, the distance between it and the deformed template surface, $\inf_{x \in S(1)} d(x, y)$, was computed. A histogram of these distances is displayed in Fig. 2d - 8d as *violin plots*. For a given distance, the thicker the plot, the greater the number of points separated by that distance. The red bar indicates the median distance.

1.4 Numerical Experiments

Three experiments were performed.

1. In the first experiment (Fig 2-4), CLARITY images were registered directly to the ABA.

2. In the second experiment (Fig 5-7), CLARITY images were registered to other CLARITY images of different conditions (e.g. Fear to Control).
3. In the third experiment (Fig 8), CLARITY images were registered to other CLARITY images within conditions (e.g. Fear to Fear).

The outputs of Image-LDDMM and Mask-LDDMM pipelines were compared to a registration pipeline written by Raju Tomer of Stanford University. Since Raju Tomer's pipeline transformed all CLARITY brains to an intermediate space, CLARITY to CLARITY transforms were computed by concatenating CLARITY to intermediate-space and intermediate-space to CLARITY transforms.

2 Results

Figures 1-8 show the registration results. Figures 2a-8a overlay the surfaces and select landmarks of the deformed template and target.

2.1 CLARITY-ABA

Figures 2-4 show the registration results of the CLARITY to ABA registrations. The Mask-LDDMM pipeline consistently outperformed the Raju and Image-LDDMM pipelines for surface distances (Fig. 2d-4d) and landmark distances (Fig. 2c-4c). The Image-LDDMM pipeline's poor performance can likely be attributed to the great difference in appearance between the Nissl-stained ABA and CLARITY images. Interestingly, the Image-LDDMM pipeline consistently yielded higher MI values than Mask-LDDMM and Raju pipelines (Fig. 2b-4b).

2.2 CLARITY-CLARITY of different conditions

Figures 5-7 show the registration results of CLARITY to CLARITY registrations. Image-LDDMM had higher MI values than Mask-LDDMM and Raju's method outperformed both Image and Mask-LDDMM (Fig. 5b-7b) in MI. For the landmark distances, Raju's method outperformed Image-LDDMM in two out of three cases (Fig. 5c, 6c). Mask-LDDMM, Image-LDDMM and Raju's method gave similar surface distances results (Fig. 5d-7d).

2.3 CLARITY-CLARITY within conditions

Figure 8 show the registration results of a CLARITY to CLARITY registration within a condition. As in the inter-condition registrations Image-LDDMM yielded better MI values than Mask-LDDMM. But unlike the inter-condition registrations, Image-LDDMM outperformed Raju's method in both MI and landmark distances (Fig. 8b-c). Once again Mask-LDDMM, Image-LDDMM and Raju's method had similar surface distances results (Fig. 8d).

3 Conclusion

In conclusion, the Mask-LDDMM pipeline outperformed both the Image-LDDMM and Raju Pipelines in aligning CLARITY brains to the ABA. The Image-LDDMM and Raju pipelines gave comparable results when transforming CLARITY images to other CLARITY images.

Raju Tomer’s method gave better results in CLARITY-CLARITY transforms between conditions. Image-LDDMM outperformed Raju’s method in a CLARITY-CLARITY transform within a condition. There are some limitations to these findings. Since CLARITY-CLARITY transforms for Raju’s Pipeline were computed by combining transforms from two registrations, additional errors that were not in the Image-LDDMM or Mask-LDDMM pipelines may have been introduced. Furthermore human error in landmark placement may have contributed to these results.

A Instructions for Visualizing using ITK-SNAP

Images and deformed ABA annotations at $25 \mu m$ resolution are found in the Google Drive in `/Tomer15/Data/kwameAlignedBrains.zip`. The [Subject].img files are the CLARITY images. The abaLabelsTo[Subject]_Raju.img and abaLabelsTo[Subject]_Kwame.img files are the ABA annotations from the Raju and Mask-LDDMM pipelines respectively.

To Install ITK-SNAP

- Download it from <http://www.itksnap.org/pmwiki/pmwiki.php?n=Downloads.SNAP3>

To open image

- File → Open Grayscale Image → Browse
- Select file
- Next → Finish

To adjust image contrast

- Tools → Image Contrast
- Drag circles in “Curve Based Adjustment”

To overlay labels on image

- Segmentation → Load From Image → Browse
- Select file
- Next → Finish

To adjust label opacity

- In the segmentation options box in the left panel, adjust the “overall label opacity”

References

- [1] <http://brain-map.org/>
- [2] Woods RP, Grafton ST, Holmes CJ, Cherry SR, Mazziotta JC. Automated Image Registration: 1. General Methods and Intrasubject Intramodality Validation. *Journal of Computer Assisted Tomography*, 22(1): 139-152.
- [3] Beg MF, Miller MI, Troué A, Younes L. Computing Large Deformation Metric Mappings via Geodesic Flows of Diffeomorphisms. *International Journal of Computer Vision*, 61(2): 139-157.
- [4] HJ Johnson, McCormick MM, Ibáñez L *et al.* The ITK Software Guide Book 1: Introduction and Development Guidelines Fourth Edition.

B Supplementary Figures

Figure 2: Control239 to Allen Brain Atlas Registration Results

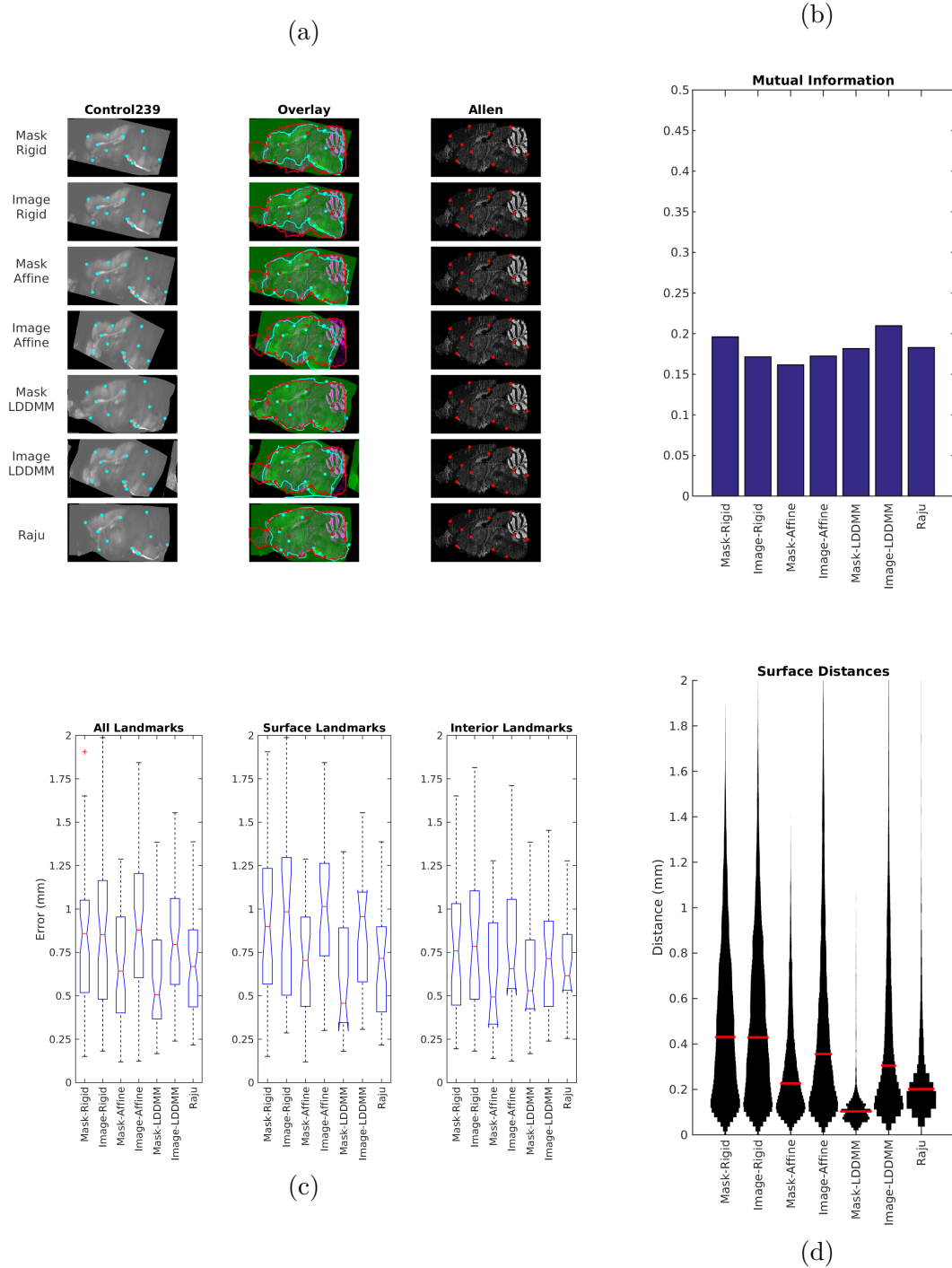


Figure 3: Cocaine178 to Allen Brain Atlas Registration Results

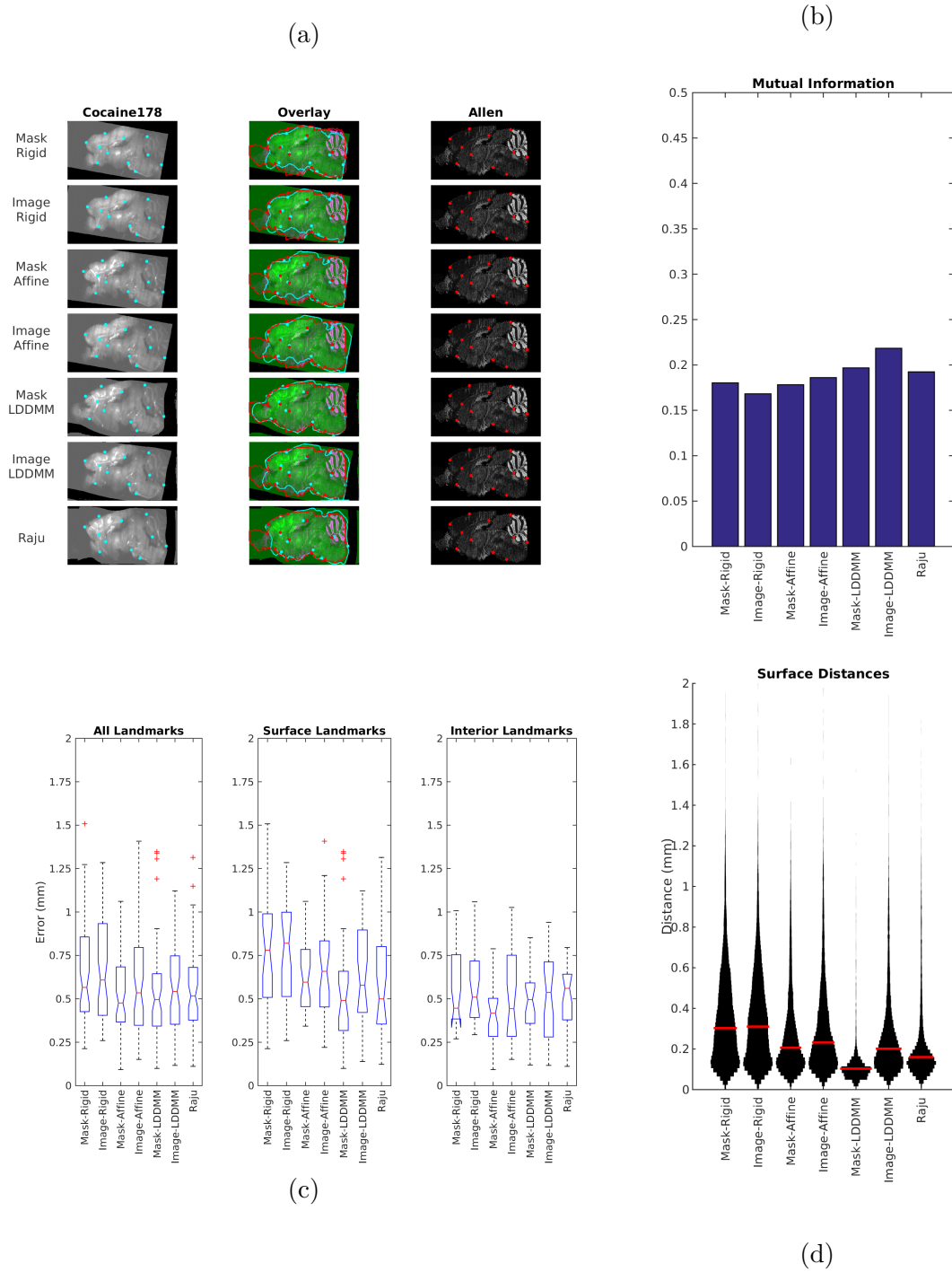


Figure 4: Fear199 to Allen Brain Atlas Registration Results

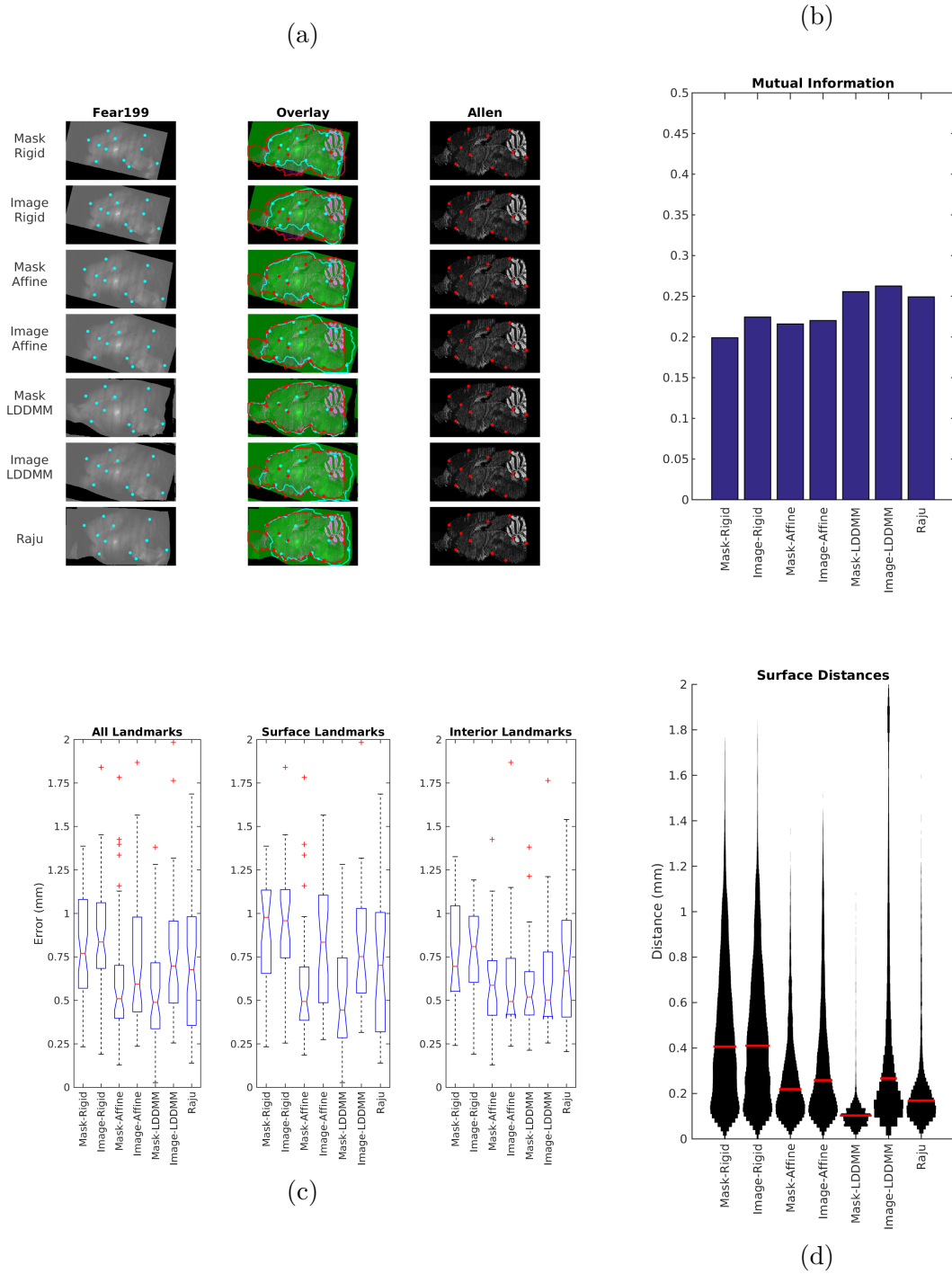


Figure 5: Cocaine178 to Control239 Registration Results

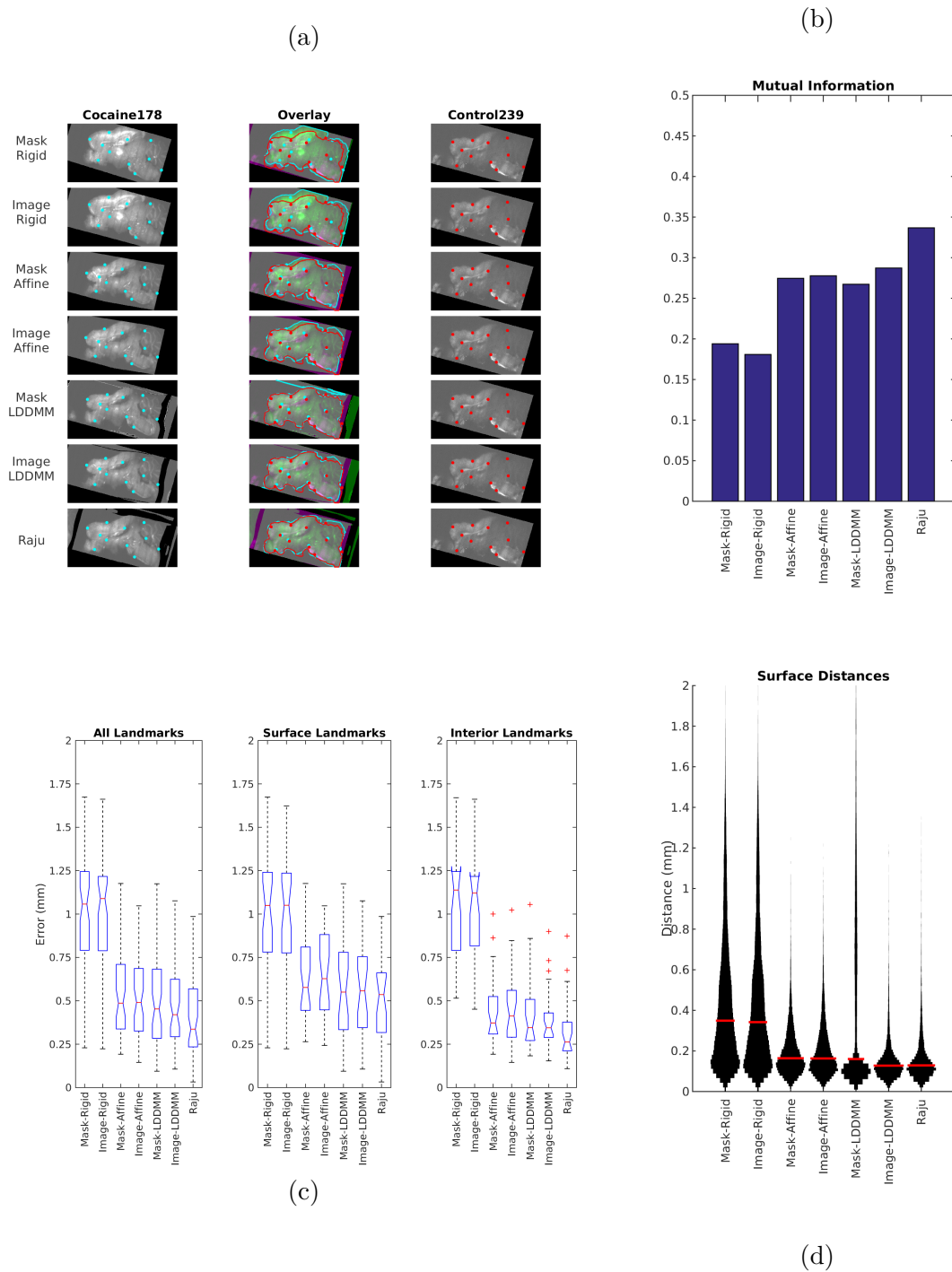


Figure 6: Fear199 to Control239 Registration Results

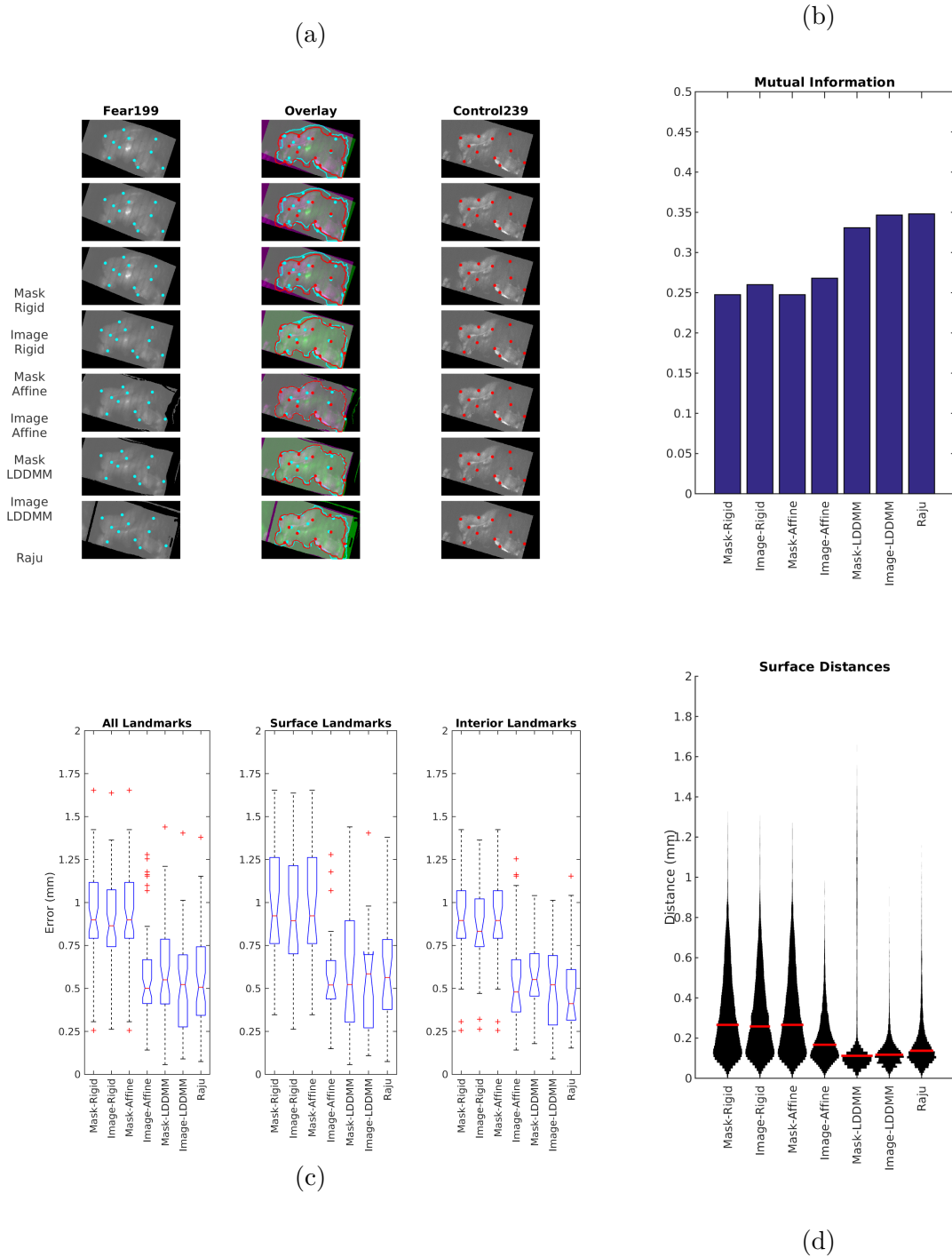


Figure 7: Fear199 to Cocaine178 Registration Results

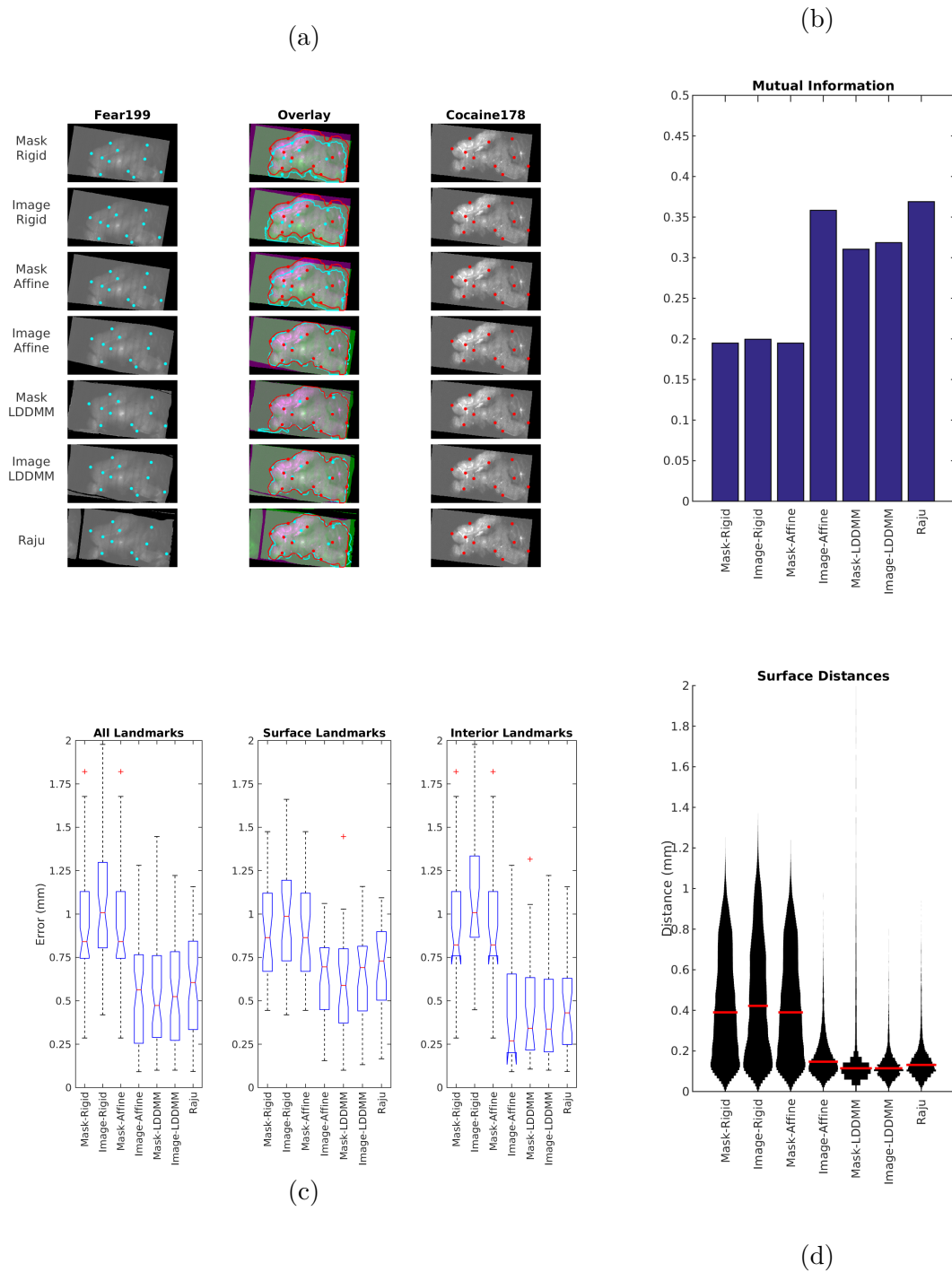


Figure 8: Fear199 to Fear188 Registration Results

